Effects of backbone rigidity on the local structure and dynamics in polymer melts and glasses

ARTICLE *in* PHYSICAL CHEMISTRY CHEMICAL PHYSICS · MARCH 2013

Impact Factor: 4.49 · DOI: 10.1039/c3cp43737j · Source: PubMed

Rajeev Kumar

Oak Ridge National Laboratory

Bobby Sumpter

Oak Ridge National Laboratory

Vladimir N Novikov

Oak Ridge National Laboratory

PCCP

RSC Publishing

PAPER

Effects of backbone rigidity on the local structure and dynamics in polymer melts and glasses

Cite this: *Phys. Chem. Chem. Phys.*, 2013, **15**, 4604

Rajeev Kumar,*[a] Monojoy Goswami,[b] Bobby G. Sumpter,[c] Vladimir N. Novikov[de] and Alexei P. Sokolov[de]

Received 23rd October 2012, Accepted 28th January 2013

DOI: 10.1039/c3cp43737j

www.rsc.org/pccp

Frustration in chain packing has been proposed to play an important role in thermodynamic and dynamic properties of polymeric melts and glasses. Based on a quantitative analysis using Voronoi tessellations and large scale molecular dynamics simulations of flexible and semi-flexible polymers, we demonstrate that the rigid polymer chains have higher averaged Voronoi polyhedral volumes and significantly wider distribution of the volume due to frustration in the chain packing. Using these results, we discuss the advantage of the rigid polymers for possible enhancement of transport properties, *e.g.* for enhancing ionic conductivity in solid polymer electrolytes.

I. Introduction

Development of low cost advanced materials for various energy applications have led to the use of polymers in lithium ion batteries,[1] organic photovoltaics,[2,3] supercapacitors,[4] fuel cells[5,6] and lightweight materials with strong mechanical properties.[7,8] In addition to the incentive of lower cost in comparison with inorganic systems such as silicon, polymer matrices provide better mechanical flexibility and significantly lighter structure, a primary requirement for many applications. A fundamental understanding of the structure–property relationship for the polymers is a prerequisite to an efficient design and synthesis of polymeric materials. However, we are still far from the microscopic understanding how chemical structure of polymers affects their macroscopic properties.

For applications such as batteries and fuel cells, a fundamental understanding of the role of chain structure and rigidity on the ion transport through the polymer matrix is of paramount importance.[1,9,10] It has also been suggested that chain rigidity affects packing of polymeric molecules and steepness of the temperature dependence of its structural relaxation (fragility).[9–15] In particular, it is predicted[15] that the backbone bending energy and cohesive interaction energy affect the fragility and glass transition temperature in a significant manner. However, a systematic study of the chain packing in polymer melts and glasses is needed to address these questions.

One of the interesting questions is the role of chain rigidity in ionic transport in polymer electrolytes. It seems obvious that more flexible polymers will have faster segmental dynamics and that leads to faster ion diffusion. However, there are several papers emphasizing strong decoupling of ionic motion from segmental dynamics in rigid polymers.[9,10,16–18] Moreover, surprisingly high ionic conductivity was reported for some rigid polymers even at temperatures below the glass transition T_g,[17,18] where ionic conductivity is expected to be negligibly small. Based on the current understanding of polymer dynamics and decoupling phenomena,[12,14,19] the authors of ref. 9 and 10 proposed an interesting scenario: flexible chains usually have good packing, low fragility and strong coupling of diffusion to structural relaxation, while rigid chains create significant frustration in packing that leads to high fragility and extreme decoupling of ion diffusion from structural relaxation. The analysis presented in ref. 10 indeed reveals a significant increase in decoupling of ionic conductivity from segmental dynamics with increase of fragility and chain rigidity. This result suggests a new way to design solid polymer electrolytes that might be based on rather rigid polymers. However, the role of chain rigidity in fragility and packing of polymer molecules remains a poorly studied topic.

The main goal of the present paper is to analyze the role of chain rigidity in packing efficiency and fragility of a polymer. In general, chain packing depends on the chemical nature of the polymer, rigidity and bulkiness of its backbone and side groups. For a chain without side groups, two key experimental

[a] *National Center for Computational Sciences, Oak Ridge National Laboratory, Oak Ridge, TN-37831, USA. E-mail: kumarr@ornl.gov*
[b] *Computer Science and Mathematics Division, Oak Ridge National Laboratory, Oak Ridge, TN-37831, USA*
[c] *Center for Nanophase Materials Sciences, Oak Ridge National Laboratory, Oak Ridge, TN-37831, USA*
[d] *Department of Chemistry, University of Tennessee, Knoxville, TN-37996, USA*
[e] *Chemical Sciences Division, Oak Ridge National Laboratory, Oak Ridge, TN-37831, USA*

variables are the temperature and the backbone rigidity.[1–3] To account for these variables, we have used the Large-scale Atomic/Molecular Massively Parallel Simulator[20] (LAMMPS) to perform the molecular dynamics (MD) simulations[21–25] of flexible and semi-flexible polymer melts and glasses. Chain packing is quantified using the Voronoi[26–34] tessellation scheme on the configurations obtained from the MD runs. This paper is organized as follows: simulation details are presented in Section II followed by results and discussion in Section III. Our conclusions are presented in Section IV.

II. Simulation details

The polymer chains are modeled by the Kremer–Grest bead-spring model.[21] The Langevin equation, $m\ddot{\boldsymbol{r}}_i = -\zeta\dot{\boldsymbol{r}}_i - \nabla_{ri}U(\{\boldsymbol{r}_i\}) + f_i(t)$, is integrated using the velocity Verlet algorithm, where m and ζ are the mass and the friction coefficient for the beads, respectively. $f_i(t)$ is the random force acting on each bead at time t and is white noise with zero mean. $U(\{\boldsymbol{r}_i\})$ is the pairwise interaction potential and is given by $U(\{\boldsymbol{r}_i\}) = U_{\mathrm{LJ}}(\boldsymbol{r}_{ij}) + U_{\mathrm{FENE}}(\boldsymbol{r}_{ij})$, where U_{LJ} is the *truncated and shifted* Lennard-Jones (LJ) potential. Explicitly, it is given by

$$U_{\mathrm{LJ}}(\boldsymbol{r}_{ij}) = \begin{cases} 4\varepsilon\left[\left(\dfrac{\sigma}{r_{ij}}\right)^{12} - \left(\dfrac{\sigma}{r_{ij}}\right)^{6} + \dfrac{1}{4}\right], & r_{ij} \leq 2.5\sigma \\ 0, & r_{ij} \geq 2.5\sigma. \end{cases}$$

Note that the exponent 12 for the repulsive part of the LJ potential falls in the limits of 9–20 estimated by density scaling analyses.[35]

The finite extensible nonlinear elastic (FENE) potential is used in combination with the Lennard-Jones potential to maintain the topology of the molecules. Explicitly, U_{FENE} can be written as

$$U_{\mathrm{FENE}}(\boldsymbol{r}_{ij}) = \begin{cases} -0.5kr_{\mathrm{c}}^{2}\ln\left[1 - \left(\dfrac{r_{ij}}{r_{\mathrm{c}}}\right)^{2}\right], & r_{ij} \leq r_{\mathrm{c}} \\ \infty, & r_{ij} \geq r_{\mathrm{c}} \end{cases},$$

such that r_{c} is the maximum extent of a bond. Here, we have used the notation $r_{ij} = |\boldsymbol{r}_{ij}|$. Following ref. 21, we have chosen $r_{\mathrm{c}} = 1.5\sigma$, $k = 30\varepsilon/\sigma^2$, $\zeta = 0.1/\hat{t}$, where $\hat{t} = \sigma\sqrt{m/\varepsilon}$ is the parameter used to quantify time steps. Results presented in this paper were obtained by carrying out the simulations in dimensionless units so that $r_{\mathrm{c}}^* = r_{\mathrm{c}}/\sigma = 1.5$, $k^* = k\sigma^2/\varepsilon = 30$, $\zeta^* = \zeta\hat{t} = 0.1$ and $\varepsilon^* = \varepsilon$ so that explicit values of ε, σ and m are needed to switch from dimensionless units to the real units.

The simulations are performed in the NPT ensemble using a Berendsen barostat[36] with the pressure fixed at $P^* = 0.001$. Usage of the Berendsen barostat for controlling the pressure is motivated by its efficiency and the fact that it gives the same results as obtained using the Andersen–Hoover barostat.[37] Periodic boundary conditions are used for two sets of chains: freely jointed chains and the chains with angular potentials. Each set contains 2000 chains and 64 beads per chain. For the second set, we have used the *harmonic* angular potential to constrain the angle between adjacent bonds. Explicitly, the angular potential used in this work is written as $U_{\mathrm{H}} = \dfrac{K_\theta}{2}[\theta - \theta_0]^2$. Simulation results presented here were obtained by choosing $K_\theta = 10\varepsilon$ and $\theta_0 = 2\pi/3$ (in radians), which is sufficient to preserve the physics of chain stiffness. For example, inclusion of angular potential leads to a change in the Flory characteristic ratio[38] defined as $C_N = \dfrac{\langle R^2\rangle}{(N-1)\sigma^2}$, $\langle R^2\rangle$ being the mean-square end-to-end distance of a chain, from $C_N = 1.62$ to $C_N = 2.82$ at $T^* = 0.8$. For the worm-like chain model,[38] $C_{N\to\infty} = \dfrac{1+\cos\theta}{1-\cos\theta}$ where θ is the angle between adjacent bond vectors and a value of $C_{N\to\infty} = 3$ is expected for $\theta = \pi/3$ corresponding to a bond angle of $2\pi/3$. It is well-known[38] that C_N increases with N and our values for the characteristic ratios are close to the estimates from the worm-like chain model. Also, we can estimate persistence length[38] (l_{p}) from the worm-like chain model as $l_{\mathrm{p}} = -\sigma/\ln\cos\theta = 1.44\sigma$ for $\theta = \pi/3$. Note that real polymers[38] have $C_{N\to\infty} > 4$ and our finite chains are reasonable models of these polymers. Also, the characteristic ratio and radius of gyration (R_{g}) decrease upon lowering the temperature. For the whole temperature range studied in this work, ratio $R_{\mathrm{g}}/R_{\mathrm{go}}$, $R_{\mathrm{go}}{}^2 = (N-1)\sigma^2/6$ being the radius of gyration of a Gaussian coil containing $N - 1$ Kuhn segments varies between 1.17–1.24 and 1.35–1.62 for the chains without and with the angular interactions, respectively. All of these results are in agreement with other simulation studies.[39,40]

Temperature in the simulations is controlled using the Langevin thermostat through the friction coefficient ζ^*. The two sets of chains are simulated at several different temperatures so that $T^* = k_{\mathrm{B}}T/\varepsilon \leq 1$. Simulations started from chains which are generated randomly in a box. Overlaps of the beads are avoided by (a) creating the initial simulation setup so that the monomers are not allowed to sit within a cut-off distance ($\sim\sigma$) and (b) by running the simulation with "soft potential" used in ref. 21 initially to spread out the monomers. After these pre-equilibration steps, switch to the LJ potential is made. For some of the low temperatures, the system gets stuck in a structurally heterogeneous state having localized dense regions next to empty spaces. However, we have found the size and shape of the structural inhomogeneity to be dependent on the initial configuration used for starting the simulations. Due to the extremely long relaxation times (from *a posteriori* analysis), it is very difficult to get rid of these inhomogeneities by isothermal relaxation. However, upon starting from a pre-equilibrated system, no such structural inhomogeneity shows up. For these cases (found to be below the glass transition temperature), we gradually decreased the temperature of a pre-equilibrated system using the Langevin thermostat at a cooling rate of $\Delta T^*/T^* = 1.0$ in one million time steps. The system is then allowed to equilibrate for around 200 million timesteps before the final production run.

To quantify chain packing, Voronoi tessellations[26–34] are used on the configurations obtained from the MD runs. The shape and volume of the Voronoi polyhedra are highly sensitive to the conformations of the chains. Both the instantaneous and average properties of the Voronoi polyhedra such as the volume and shape are analyzed. Furthermore, the conformational degrees of freedom of the chains depend on the intra- and interchain interactions in a complicated manner. The MD simulation procedure described above allows us to study the effects of these interactions on the distribution of the Voronoi polyhedra in the melts and glasses as a function of temperature and backbone rigidity.

III. Results and discussion

In Fig. 1(a), we present the computed average Voronoi volume as a function of temperature for the two sets of chains. We have found that after equilibration the average of polyhedra volumes shown in Fig. 1(a) is independent of the number of configurations averaged over within errors. Also, the average Voronoi volume is found to be the same as the specific volume which is a direct consequence of the space-filling nature of the Voronoi tessellation scheme. An increase in the specific volume with an increase in temperature is an outcome of thermal expansion, captured by our simulations in the NPT ensemble. The change in the slope of the specific volume curve with an increase in the temperature such as those seen in Fig. 1(a) is used to locate the glass transition temperature (T_g).[41] However, the change in the specific volume with temperature is somewhat sensitive to the cooling rate[41] and the results for T_g are dependent on the cooling rate. In this work, we have used the same cooling rate for the two sets of chains for the comparison purposes. It is clear from Fig. 1(a) that the chains with angular potential have higher glass transition temperature ($T_g \sim 0.644$) in comparison with the chains without any angular potential ($T_g \sim 0.4$). This is in qualitative agreement with experimental results,[19] predictions of the generalized entropy theory[42] and a similar molecular dynamics study.[37] Furthermore, the averaged Voronoi volume *below* T_g is found to be larger for rigid chains. Realizing that $\sim$5% difference in densities corresponds to a significant change in packing, these results show that the chains with angular potentials have significantly larger volume.

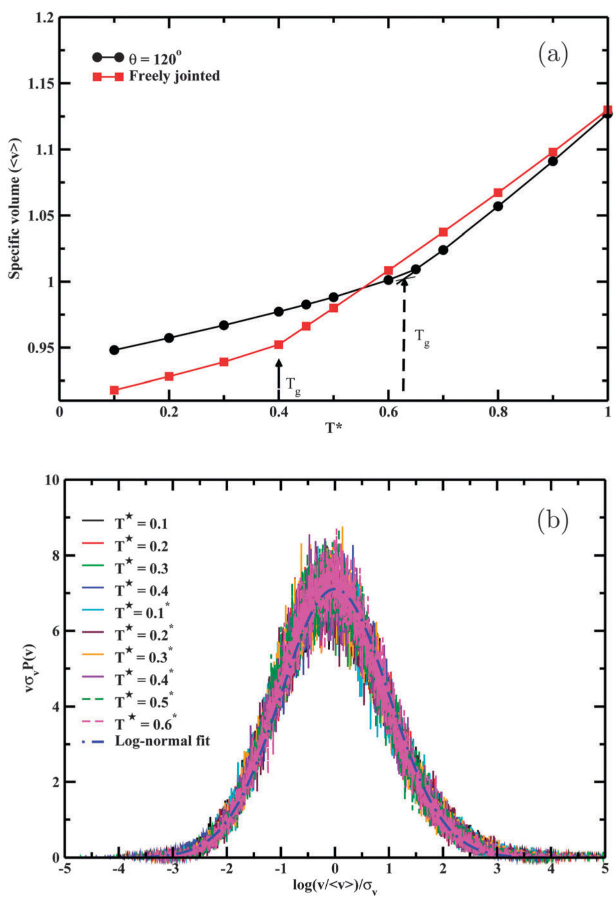

Fig. 1 Specific volume ($\langle v \rangle$) obtained at different temperatures for the two sets of chains is shown in (a). Distributions/histograms of the Voronoi polyhedra volumes (b) for temperatures below the glass-transition temperature (T_g defined in (a)) fall on a master curve, which fits the log-normal distribution function. Plots with * represent the chains with angular potential and $\sigma_\nu = \sqrt{\langle \nu^2 \rangle - \langle \nu \rangle^2}$ is the standard deviation.

The shape of the probability distribution function of the Voronoi volume has been a topic of discussion in free-volume theories.[43] Also, the shape is very important for fitting protocols used in simulations[31] while extracting different parameters such as effective hard-sphere radius for the Lennard-Jones systems. Furthermore, the distribution function is found to have a universal shape in the glassy regime explored using simulations[29] for similar systems containing shorter chains (100 chains containing 20 beads per chain) in the NVT ensemble. In order to relate our work to these directions of research, we have tried to fit our numerical data with different widely used shapes (normal, two and three parameter gamma function) of the distribution functions. It is found that log-normal distribution (which is one of the "maximum information entropy" distribution[44]) fits our data (Fig. 1(b)) better than the normal distribution (which is another "maximum information entropy" distribution) and gamma distributions for temperatures equal to or below the glass transition temperature, independent of the angular potential. This observation is in agreement with the simulation study[29] by Starr *et al.* In the literature, deviation of the Voronoi volume distribution from the gamma and normal/Gaussian probability distribution function is attributed to correlations[33] and strong density fluctuations[45] from their equilibrium values, respectively. This, in turn, implies that there are strong correlations and density fluctuations in the glassy region, as expected. The universal nature of the shape of the distribution function in the glassy region is confirmed by plotting all of the numerical data on a master curve corresponding to the log-normal distribution function. From Fig. 1(b), it is found that all of our data (averaged over 1000 configurations) follows the same master curve.

In order to highlight differences between short-time/instantaneous and long-time averaged distributions of the Voronoi volumes, we have computed the distributions after averaging over an increasing number of configurations spanning longer time. As an example, we show (Fig. 2(a)) the distribution of the Voronoi volumes for $T^* = 1.0$ as a function of the number of configurations used for averaging the chains with angular potential.

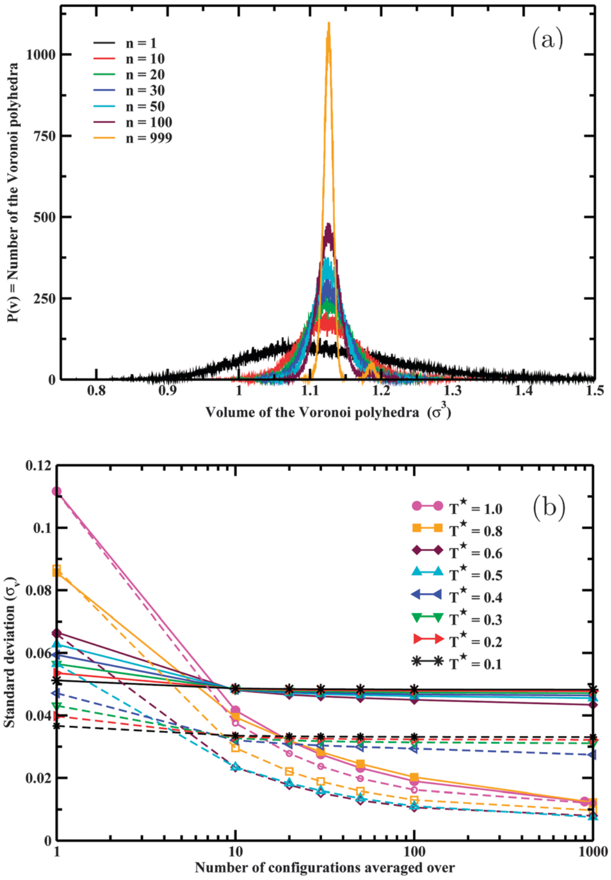

Fig. 2 Distribution of the Voronoi polyhedra volume in the melts containing the chains with angular potentials for $T^* = 1.0$. Effect of chain dynamics on the distribution is observed through the change with the number of configurations used for averaging (n). Standard deviation, a measure for the width of the distribution, is also dependent on n, as shown in (b). Solid and dashed lines represent the chains with and without the angular potentials, respectively.

For a low number of configurations used for averaging ($n \leq 50$), there is only one broad peak and upon increasing the number of configurations used for averaging, the peak narrows and an extra peak shows up. We have found the same behavior for all the other cases above T_g. The additional peak at higher volumes arises from the chain ends. This is in agreement with an early study in the NVT ensemble.[26] Physically, this means that the chain ends have higher free volume. In contrast, the distribution more or less stays the same independent of the number of configurations used for averaging in the glassy region.

Dependence of the distribution of the Voronoi volume on the averaging time is also seen to affect the width of the distribution. In Fig. 2(b), we show the standard deviation, $\sigma_\nu = \sqrt{\langle \nu^2 \rangle - \langle \nu \rangle^2}$, as a function of the number of configurations averaged over (*i.e.*, as time). The standard deviation decreases with an increase in the number of configurations averaged over all the temperatures. However, the change is much smaller for lower temperatures, especially below T_g. Note that the standard deviation is higher for the chains with angular potentials for the same temperature. Our current understanding[1] about the transport of molecules and ions through the polymer matrix relies on the extent of "free volume". Quantitative relation between the Voronoi volume and "free volume" does not exist due to the lack of rigor in the definition of "free volume". However, qualitatively, the Voronoi volume can be interpreted as the local space available to a molecule. The observed increase in the averaged Voronoi volume and the width of the volume distribution with increase in chain rigidity indicates significant frustration in packing and higher "free volume" in the melt of more rigid chains. We emphasize that the observed large decrease ($\sim$5%) in density alone creates significant free volume. Moreover, the revealed increase in the width of the Voronoi volumes distribution by almost 50% at T^* close to T_g (Fig. 2(b)) suggests the existence of rather porous structures of the rigid chains. In classical theory, ions in a polymer can diffuse only when surrounding segments are moving. This leads to a coupling of ionic conductivity to segmental dynamics which is usually observed in flexible polymers like poly(ethylene oxide) (PEO). However, the existence of rather porous not well-packed structure might provide enough space for diffusion of small ions even when segmental dynamics is very slow or completely frozen. Thus, the presented results provide a possible microscopic picture behind the strong decoupling of ionic conductivity from segmental dynamics reported in several studies of rigid polymers.[9,10,16–18] We emphasize that frustration in chain packing alone is not sufficient for high ionic conductivity, but this might be a critical factor in employing the decoupling phenomena and creating a "superionic" polymer.

The observed dependence of the distribution on the number of configurations (Fig. 2(b)) is expected when we take into account the fact that the structural relaxation time increases by orders of magnitude when temperature is lowered below T_g. To quantify the structural relaxation time, for the two sets of chains, we have computed the incoherent scattering function[22] (Fourier transform of the self part of the van-Hove correlation function) for wavevectors corresponding to the first maximum of the static structure factor. The results for the chains with angular potential are shown in Fig. 3. Slowing of the structural

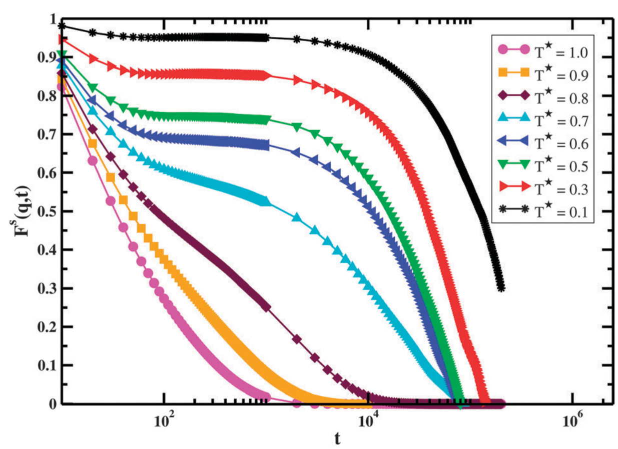

Fig. 3 Incoherent intermediate scattering functions ($F^s(\boldsymbol{q},t)$) for the chains with angular potentials are shown here. The wavevector $\boldsymbol{q}$ corresponds to the first maximum in the structure factor.

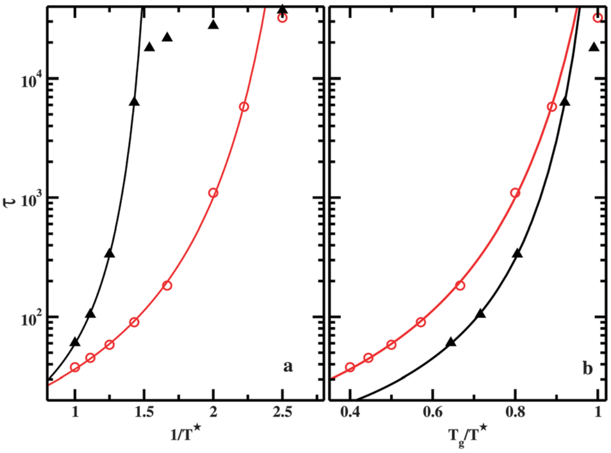

Fig. 4 (a) Temperature dependence of segmental relaxation time for rigid (triangles) and flexible (circles) chains. The solid lines present VFT fits. Only data with $\tau < 10^4$ have been used for the fit. (b) The same data presented *vs.* T_g/T^* with $T_g = 0.4$ for flexible and $T_g = 0.644$ for rigid chains. The plot demonstrates significant difference in fragility of flexible and rigid chains.

relaxation can be observed by the development of a plateau region, which starts as early as $T^* = 0.8$. We define relaxation time (τ) as the time at which the intermediate scattering function approaches $1/e$ of the maximum value (=1). The relaxation times for both chains show non-Arrhenius temperature variations (Fig. 4(a)) that can be fit by the traditional Vogel–Fulcher–Tammann (VFT) relation[46,47] $\left(\tau = \tau_0 \exp\left(\dfrac{B}{T - T_0}\right)\right)$, with the fit values of $\ln \tau_0 = 2.431$, $B = 0.786$, $T_0 = 0.325$ and $\ln \tau_0 = 2.166$, $B = 0.813$, $T_0 = 0.576$ for the chains in the absence and presence of angular potentials, respectively. We emphasize that in this fit we only used points with $\tau < 10^4$ to exclude any non-equilibrium effects in our analysis. As it is obvious from Fig. 4(a), the system falls off equilibrium at longer τ.

Comparison of the relaxation behavior using the fragility plot (Fig. 4(b)) suggests that the more rigid chain has steeper temperature dependence of structural relaxation, *i.e.* higher fragility. The fragility index can be estimated using the definition[48] as $m(T^*) = \mathrm{d}(\log(\tau))/\mathrm{d}(T_g/T^*)_{|T_g/T^*=1}$. Using the parameters of the VFT fits (Fig. 4), we estimate the fragility index to be $m \sim 24$ for flexible chains at $T_g = 0.4$ and $m \sim 50$ for rigid chains at $T_g = 0.644$. These values of the fragility indices agree with the empirical findings[11,47] that polymers with rigid backbones are highly fragile. We are not aware of any explicit proof of these empirical findings and our simulations provide a quantitative support to these observations for the first time.

IV. Conclusions

In summary, we have demonstrated that polymer backbone rigidity affects the T_g and distribution of the Voronoi polyhedra volumes in the polymeric melts and glasses. We have found that the distribution in the glassy region is log-normal and universal in nature. The distribution for the rigid chains is found to have $\sim$5% higher average value and significantly larger width in comparison with the flexible chains for all the temperatures. Comparing the averaged volume and distribution width for flexible and rigid chains at different temperatures, scaled by T_g, we found that the rigid chains have significantly higher frustration in packing at the same relaxation time. The observed frustration in packing is in agreement with the experimental finding that the polymers showing highest gas permeability[49] have rigid backbones (polyacetylenic). The observed effects of backbone rigidity on the relaxation times are in qualitative agreement with a recent work by Colmenero *et al.*[50] It is expected[1] that frustration in packing also affects the transport of ions in polymer electrolytes: a poorly packed structure provides the possibility for ion transport to be strongly decoupled from segmental dynamics. Thus the use of relatively rigid polymers might be beneficial for use in many applications, including batteries and fuel cells. For example, our study points out that flexible macromolecules like poly(ethylene oxide) (PEO) having $T_g \sim 232$ K, *i.e.*, below room temperature, will have less frustration in packing (*i.e.*, low averaged Voronoi volume) compared to rigid polymers and hence, strong coupling between ionic diffusion and segmental dynamics. This is indeed observed experimentally.[9,10] The extent of the decoupling can be tuned by increasing the backbone rigidity.[9,10] A wider distribution of the averaged Voronoi volume at lower temperatures might be a key for high ionic conductivity. Keeping this in mind, our results show that polymeric materials with rigid backbones might provide an alternative way to design polymer electrolytes with high ionic conductivity. Recently published experimental results[9,10,18] are in agreement with this idea. Furthermore, our results confirm the theoretical predictions and empirical observations that rigid polymers are highly fragile.

In the end, we comment on an apparent but non-trivial connection between our work related to the Voronoi volume distribution and the positron annihilation spectroscopy (PAS) studies[51–55] quantifying "free volume" distributions in polymers. As mentioned earlier, the Voronoi volume can be interpreted (qualitatively) as the "free volume" available to its centroid. However, there is no unambiguous way[29] of quantifying "free volume" from a Voronoi study. In addition, the measurement of the positron lifetime distribution might lead to a distorted "free volume" distribution in certain cases, *e.g.*, calculated "free volume" distributions are shifted to higher values.[52,54] So, using PAS for comparison with the Voronoi tessellation requires separate careful investigation. We expect that relations[29] between the Debye–Waller factor obtained directly from the mean square displacement data and free volume may be more suitable for such a comparison.

Acknowledgements

MG, BGS and APS acknowledge financial support from the Division of Materials Science and Engineering, U.S. Department of Energy, Office of Basic Energy Sciences. RK acknowledges support from the Oak Ridge Leadership Computing Facility at the Oak Ridge National Laboratory, which is supported by the Office of Science of the U.S. Department of Energy under

Contract No. DE-AC05-00OR22725. Also, we acknowledge support from UT-Battelle through the LDRD program (project #05608) during initial stages of this work.

References

1 F. M. Gray, *Solid Polymer Electrolytes: Fundamentals and Technological Applications*, VCH Publishers, Inc., New York, 1991.
2 K. M. Coakley and M. D. McGehee, *Chem. Mater.*, 2004, **16**, 4533.
3 H. Hoppe and N. S. Sariciftci, Photoresponsive Polymers II, *Adv. Polym. Sci.*, 2008, **214**, 1–86.
4 J. J. Yoo, K. Balakrishnan, J. Huang, V. Meunier, B. G. Sumpter, A. Srivastava, M. Conway, A. L. M. Reddy, J. Yu, R. Vajtai and P. M. Ajayan, *Nano Lett.*, 2011, **11**, 1423.
5 S. M. J. Zaidi and T. Matsuura, *Polymer Membranes for Fuel Cells*, Springer Science + Business Media, LLC, New York, 2009.
6 H. Zhang and P. K. Shen, *Chem. Rev.*, 2012, **112**, 2780.
7 A. V. Ruzette and L. Leibler, *Nat. Mater.*, 2005, **4**, 19.
8 S. K. Kumar and R. Krishnamoorti, *Annu. Rev. Chem. Biomol. Eng.*, 2010, **1**, 37.
9 A. L. Agapov and A. P. Sokolov, *Macromolecules*, 2011, **44**, 4410.
10 Y. Y. Wang, A. L. Agapov, F. Fan, K. L. Hong, X. Yu, J. Mays and A. P. Sokolov, *Phys. Rev. Lett.*, 2012, **108**, 088303.
11 K. L. Ngai and C. M. Roland, *Macromolecules*, 1993, **26**, 6824.
12 J. Dudowicz, K. F. Freed and J. F. Douglas, *J. Phys. Chem. B*, 2005, **109**, 21350.
13 J. Dudowicz, K. F. Freed and J. F. Douglas, *Adv. Chem. Phys.*, 2008, **137**, 125.
14 A. P. Sokolov and K. S. Schweizer, *Phys. Rev. Lett.*, 2009, **102**, 248301.
15 E. B. Stukalin, J. F. Douglas and K. F. Freed, *J. Chem. Phys.*, 2009, **131**, 114905.
16 H. Sasabe and S. Saito, *Polym. J. (Tokyo)*, 1972, **3**, 624.
17 X. Wei and D. F. Shriver, *Chem. Mater.*, 1998, **10**, 2307.
18 C. T. Imrie, M. D. Ingram and G. S. McHattie, *J. Phys. Chem. B*, 1999, **103**, 4132.
19 K. Kunal, C. G. Robertson, S. Pawlus, S. F. Hahn and A. P. Sokolov, *Macromolecules*, 2008, **41**, 7232.
20 S. Plimpton, *J. Comput. Phys.*, 1995, **117**, 1, http://lammps.sandia.gov.
21 K. Kremer and G. S. Grest, *J. Chem. Phys.*, 1990, **92**, 5057.
22 K. Binder, J. Baschnagel and W. Paul, *Prog. Polym. Sci.*, 2003, **28**, 115.
23 J. L. Barrat, J. Baschnagel and A. Lyulin, *Soft Matter*, 2010, **6**, 3430.
24 T. S. Jain and J. J. de Pablo, *J. Chem. Phys.*, 2005, **122**, 147515.
25 R. S. Hoy and M. O. Robbins, *Phys. Rev. E: Stat. Phys., Plasmas, Fluids, Relat. Interdiscip. Top.*, 2008, **77**, 031801.
26 D. Rigby and R. J. Roe, *Macromolecules*, 1990, **23**, 5312.
27 M. L. Greenfield and D. N. Theodorou, *Macromolecules*, 1993, **26**, 5461.
28 A. Okabe, B. Boots, K. Sugihara and S. N. Chiu, *Spatial Tessellations: Concepts and Applications of Voronoi Diagrams*, Wiley, New York, 2000, Wiley Series in Probability and Statistics.
29 F. W. Starr, S. Sastry, J. F. Douglas and S. C. Glotzer, *Phys. Rev. Lett.*, 2002, **89**, 125501.
30 M. Sega, P. Jedlovszky, N. N. Medvedev and R. Vallauri, *J. Chem. Phys.*, 2004, **121**, 2422.
31 V. S. Kumar and V. Kumaran, *J. Chem. Phys.*, 2005, **123**, 114501.
32 C. H. Rycroft, G. S. Grest, J. W. Landry and M. Z. Bazant, *Phys. Rev. E: Stat. Phys., Plasmas, Fluids, Relat. Interdiscip. Top.*, 2006, **74**, 16.
33 L. Zaninetti, *Phys. Lett. A*, 2009, **373**, 3223.
34 B. J. Sung and A. Yethiraj, *Phys. Rev. E: Stat. Phys., Plasmas, Fluids, Relat. Interdiscip. Top.*, 2010, **81**, 031801.
35 C. M. Roland, S. Bair and R. Casalini, *J. Chem. Phys.*, 2006, **125**, 124508.
36 H. J. C. Berendsen, J. P. M. Postma, W. F. van Gunsteren, A. DiNola and J. R. Haak, *J. Chem. Phys.*, 1984, **81**, 3684.
37 B. Schnell, H. Meyer, C. Fond, J. P. Wittmer and J. Baschnagel, *Eur. Phys. J. E: Soft Matter Biol. Phys.*, 2011, **34**, 97.
38 M. Rubinstein and R. H. Colby, *Polymer Physics*, Oxford University Press, New York, 2003.
39 D. Rigby and R. J. Roe, *J. Chem. Phys.*, 1987, **87**, 7285.
40 C. Bennemann, W. Paul, K. Binder and B. Dunweg, *Phys. Rev. E: Stat. Phys., Plasmas, Fluids, Relat. Interdiscip. Top.*, 1998, **57**, 843.
41 J. Buchholz, W. Paul, F. Varnik and K. Binder, *J. Chem. Phys.*, 2002, **117**, 7364.
42 J. Dudowicz, K. F. Freed and J. F. Douglas, *J. Phys. Chem. B*, 2005, **109**, 21285.
43 M. H. Cohen and G. S. Grest, *Phys. Rev. B: Condens. Matter Mater. Phys.*, 1979, **20**, 1077.
44 E. T. Jaynes, *Phys. Rev.*, 1957, **106**, 620.
45 T. S. Chow, *Macromol. Theory Simul.*, 1995, **4**, 397.
46 J. Rault, *J. Non-Cryst. Solids*, 2000, **271**, 177.
47 A. P. Sokolov, V. N. Novikov and Y. Ding, *J. Phys.: Condens. Matter*, 2007, **19**, 205116.
48 C. A. Angell, *Science*, 1995, **267**, 1924.
49 Y. Hu, M. Shiotsuki, F. Sanda, B. D. Freeman and T. Masuda, *Macromolecules*, 2008, **41**, 8525.
50 M. Bernabei, A. J. Moreno, E. Zaccarelli, F. Sciortino and J. Colmenero, *Soft Matter*, 2011, **7**, 1364.
51 Y. C. Jean, *Microchem. J.*, 1990, **42**, 72.
52 R. M. Dammert, S. L. Maunu, F. H. J. Maurer, I. M. Neelov, S. Niemela, F. Sundholm and C. Wastlund, *Macromolecules*, 1999, **32**, 1930.
53 K. Suvegh, M. Klapper, A. Domjan, S. Mullins, W. Wunderlich and A. Vertes, *Macromolecules*, 1999, **32**, 1147.
54 K. Suvegh, M. Klapper, A. Domjan, S. Mullins and A. Vertes, *Radiat. Phys. Chem.*, 2000, **58**, 539.
55 V. P. Shantarovich, T. Suzuki, Yu. P. Yampolskii, P. Budd, V. V. Gustov, I. B. Kevdina, A. V. Pastukhov, S. S. Berdonosov and V. E. Bozhevolnov, *High Energy Chem.*, 2007, **41**, 370.

